

Analytical Multiphysics Model for NVH Prediction of a high-speed Surface-Permanent Magnet Synchronous Machine

Andreou, Panagiotis; Hajjaj, Amal; Mohammadpour, Mahdi; Theodossiades, Stephanos

Loughborough University, Epinal Way
Loughborough, LE11 3TU, United Kingdom
+44 (0) 1509 227664
S.Theodossiades@lboro.ac.uk

Keywords: Analytical Multiphysics, Electromagnetics, Vibroacoustics, E-motor, PMSM

ABSTRACT

As demands for electric motor efficiency keep increasing, Electric Vehicle (EV) manufacturers are striving to design smaller and more power-dense machines, able to maintain performance standards through high-speed operation. However, increased operating loads and speeds in excess of 10,000 rev/min results in the amplification, or introduction of new noise components, which necessitate novel prediction techniques. The use of traditional finite element (FE) based optimisation methodologies therefore becomes challenging due to extensive computational loads. In this work, an analytical multi-physics methodology for e-NVH prediction of typical high-speed Surface-mounted Permanent Magnet Synchronous Machines (S-PMSMs) is presented. The model comprises analytical electromagnetics and vibro-acoustics to determine the radiated airborne noise of SPMSMs at speeds above 10,000 rev/min and correspondingly high frequencies. Preliminary results are presented to highlight the efficiency of the proposed method.

RESUMEN

1. INTRODUCTION

With demands for EVs being at an all-time high [1], the optimisation of the performance and efficiency of electric traction motors has become a key point of focus in automotive industry. Nevertheless, such improvements often result in an amplification of the excitations of the mechanical structure and subsequently impact the NVH response of electric machines adversely. This is further exacerbated when considering the noise profile of e-motors, which can be perceived as highly annoying by the human ear due to its tonal nature at higher frequencies relative to an internal combustion engine. Thus, the NVH behaviour of the system has become a significant criterion in the early design stages of an electric traction motor.

The main components of noise generated by EV traction motors are of electromagnetic origin [2], primarily due to the time and space-varying Maxwell stresses induced at the interface between the airgap and the ferromagnetic materials [3]. These act directly on both the stator and the rotor and result in the generation of airborne and structure-borne noise. Therefore, an e-motor vibroacoustic study requires a multi-physics methodology combining electromagnetic, structural dynamics and vibroacoustic principles.

A plethora of studies can be found in literature, attempting to characterise the NVH behaviour of electric motors using numerical techniques, due to their higher fidelity [4]–[15]. These include Finite Element (FE) Electromagnetic and Structural models, as well as FE and Boundary Element models for the acoustic response of the system. Nevertheless, for high-speed electric motors whereby higher frequencies and spatial harmonics must be considered, the use of numerical methods becomes prohibitive due to the immense computational expense. For this reason, the development of a reliable reduced-order methodology that can analytically investigate potential electromagnetic and vibroacoustic issues and provide fast and valid NVH predictions is of crucial importance.

In this work, an analytical methodology used to study the NVH behaviour of a typical traction S-PMSM is presented. The Complex Permeance (CP) approach has been utilised for the resolution of the motor electromagnetics and hence, using the Maxwell Stress Tensor, the excitations acting on the stator have been computed. The stator's natural frequencies and vibration response have been calculated analytically using expressions for an equivalent 2-Dimensional ring, while airborne noise generation has been evaluated based on modal radiation efficiencies for a hollow cylindrical structure.

2. METHODOLOGY

2.1. Modelling Assumptions

The following assumptions have been employed in the method development:

- The flux variation in the axial dimension is negligible, thus considered to be two-dimensional
- The motor is in Open-Circuit Conditions (i.e. no load)
- The physical properties of the materials are constant and isotropic
- The iron core is infinitely permeable and magnetic saturation is neglected
- End effects are neglected
- The stator slots are infinitely deep
- The mutual influence between slots is ignored

2.2. Formulation

In CP, the resultant magnetic flux density in the airgap is computed as the product of the analytically calculated magnetic flux density in an equivalent slot-less topology and a complex modulating permeance function [16]:

$$\lambda^* = \lambda_a + j\lambda_b \quad (1)$$

$$B_{radial}^{slotted}(r, \theta, t) = B_{radial}^{slotless}(r, \theta, t) \lambda_a(r, \theta) + B_{tangential}^{slotless}(r, \theta) \lambda_b(r, \theta) \quad (2)$$

$$B_{tangential}^{slotted}(r, \theta, t) = B_{tangential}^{slotless}(r, \theta, t) \lambda_a(r, \theta) - B_{radial}^{slotless}(r, \theta) \lambda_b(r, \theta) \quad (3)$$

where B stands for magnetic flux density in units of Tesla, T , while λ_a and λ_b are the radial and tangential components of the complex permeance modulating function. The magnetic flux density fields were evaluated using the method outlined by *Zhu et al.* [17] while the complex function λ^* was obtained using the analytical expressions derived by *Wang et al.* [18] :

$$\lambda_a(r, \theta) = -g_1 \cdot \frac{1 + \frac{k_c - 1}{K_0} \sum_{n=1}^{\infty} [Q_n R_a(n) \cos(nZ_s \theta)]}{r \ln\left(\frac{R_s}{R_r}\right) + \frac{k_c - 1}{K_0} \frac{R_s}{Z_s} \sum_{n=1}^{\infty} \left[\frac{(-1)^n}{n} Q_n\right]} \quad (4)$$

$$\lambda_b(r, \theta) = -g_1 \cdot \frac{\frac{k_c - 1}{K_0} \sum_{n=1}^{\infty} [Q_n R_b(n) \sin(nZ_s \theta)]}{r \ln\left(\frac{R_s}{R_r}\right) + \frac{k_c - 1}{K_0} \frac{R_s}{Z_s} \sum_{n=1}^{\infty} \left[\frac{(-1)^n}{n} Q_n\right]} \quad (5)$$

where:

$$Q_n = \int_0^{\frac{\alpha_{s0}}{2}} \left(\frac{1}{\sqrt[3]{\frac{\alpha_{s0}}{2} - \theta}} - \frac{1}{\sqrt[3]{\frac{\alpha_{s0}}{2} + \theta}} \right) \sin(nZ_s \theta) d\theta \quad (6)$$

$$R_a(n) = \left(\frac{r}{R_s}\right)^{nZ_s - 1} \cdot \frac{\left[1 + \left(\frac{R_r}{r}\right)^{2nZ_s}\right]}{\left[1 - \left(\frac{R_r}{R_s}\right)^{2nZ_s}\right]} \quad (7)$$

$$R_b(n) = \left(\frac{r}{R_s}\right)^{nZ_s - 1} \cdot \frac{\left[1 - \left(\frac{R_r}{r}\right)^{2nZ_s}\right]}{\left[1 - \left(\frac{R_r}{R_s}\right)^{2nZ_s}\right]} \quad (8)$$

$$K_0 = \sum_{n=1}^{\infty} Q_n R_a(n) \cos(n\pi) \quad (9)$$

In Equations 4 – 9, θ is the mechanical angle in the airgap, R_r is the outer radius of the rotor, R_m is the outer radius of the magnets ($R_m = R_r + h_m$, where h_m is the magnet thickness), R_s is the stator's inner radius, r is the radius at the middle of the airgap, α_{s0} stands for the slot opening angle, Z_s is the number of stator slots, g_1 is the perpendicular distance between the rotor's outer surface and the stator's inner surface, $g_1 = R_s - R_r$ and k_c is the Carter coefficient. The Maxwell pressures in the middle of the airgap were evaluated through the Maxwell Stress Tensor as [19]:

$$P_{radial} = \frac{B_{radial}^{slotted^2} - B_{tangential}^{slotted^2}}{2\mu_0} \quad (10)$$

$$P_{tangential} = \frac{B_{radial}^{slotted} \times B_{tangential}^{slotted}}{\mu_0} \quad (11)$$

where μ_0 is the magnetic permeability of free space. The natural frequencies and mode shapes of the stator as well as the modal radiation efficiencies used in the vibroacoustic calculations were computed using the methods described in [2], [20]. Static and dynamic displacements as well as spatially averaged vibration velocities due to each excitation mode were computed through the method described in [21]. Finally, modal damping values were evaluated using the empirical formula described in [21]:

$$\zeta_m = \frac{1}{2\pi} (2.76 \times 10^{-5} f_m + 0.062) \quad (12)$$

where ζ_m and f_m are the damping ratio and corresponding natural frequency of mode m .

3. CASE STUDY AND RESULTS

The electric machine used for the development and assessment of the methodology is a 48-slot, 8-pole S-PMSM. A cross sectional view of the machine is shown in Figure 1, while further parameters regarding the machine are presented in Table 1. Simulations were performed on a 40-core high-performance computer, with a simulation sampling rate and total time of 100 kHz and 0.5 s respectively, for each motor speed increment, in order to obtain a fine resolution. A total of 593 speed intervals were simulated to predict with a run-time of 6:25 h, averaging at only 39 s per speed interval, for the resolution of the electromagnetic and vibroacoustic problems.

Table 1 – Main machine parameters used in methodology

Parameter	Symbol	Value	Unit
Number of Pole Pairs	p	4	–
Number of Stator Slots	Z_s	48	–
Rotor Radius	R_r	71	mm
Stator Inner Radius	R_s	82	mm
Magnet Radial Height	h_m	6	mm
Pole-Arc to Pole-Pitch Ratio	α_p	0.575	–
Magnet Remanence	B_0	1.2	T
Vacuum Permeability	μ_0	$4\pi \times 10^{-7}$	H/m
Magnet Relative Recoil Permeability	μ_r	1.04	–
Magnetisation Type	–	radial	–
Slot Opening Angle	α_{s0}	3.5	°
Slot Opening Width	b_s	5	mm
Slot Pitch Distance	t_s	10.73	mm

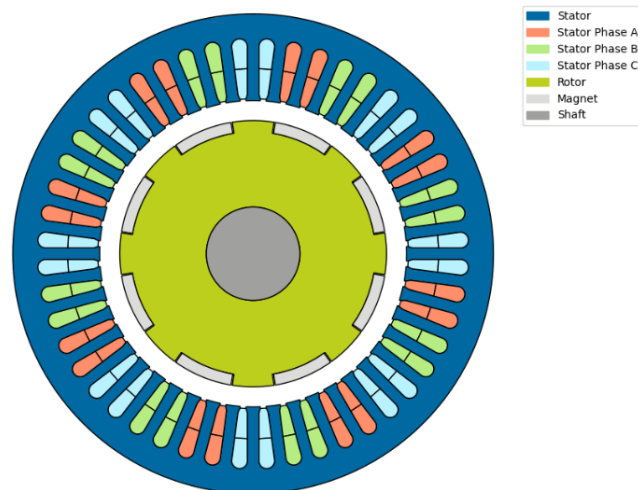


Figure 1 - Cross-sectional view of the case study e-motor.

The radial and tangential components of the magnetic flux density field in the middle of the airgap are presented in Figure 2. These results have been validated against literature as well as numerical electromagnetic modelling.

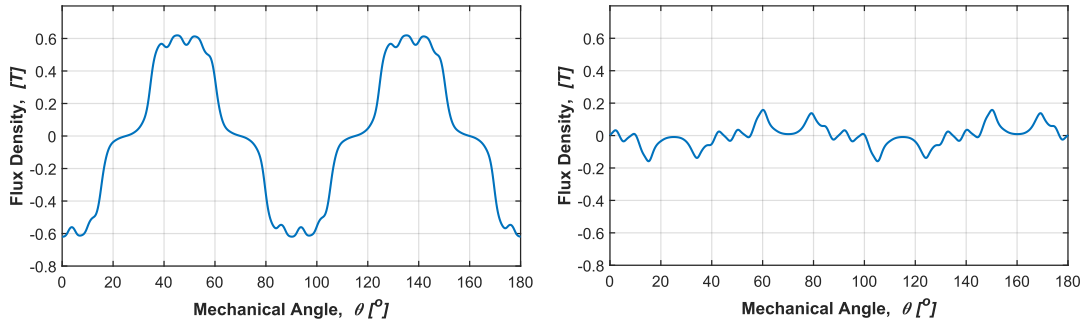


Figure 2 – Radial (left) and tangential (right) flux density distribution in the airgap (right)

The two-dimensional decomposition of the forces acting on the stator is presented in Figure 3, with the main force components being multiples of twice the electrical supply frequency and multiples of $2p$ in the spatial harmonic content. Negative spatial orders represent waves travelling in the opposite direction than the rotation of the rotor and have also been considered. The predicted Sound Pressure Levels presented in Figure 4 highlight the presence of these harmonics in the airborne noise spectrum. Lastly, the resonance effects between the excitation forces and the breathing mode (2190 Hz) and 8th circumferential mode of the stator (10,400 Hz) are shown as vertical lines on the SPL spectrum.

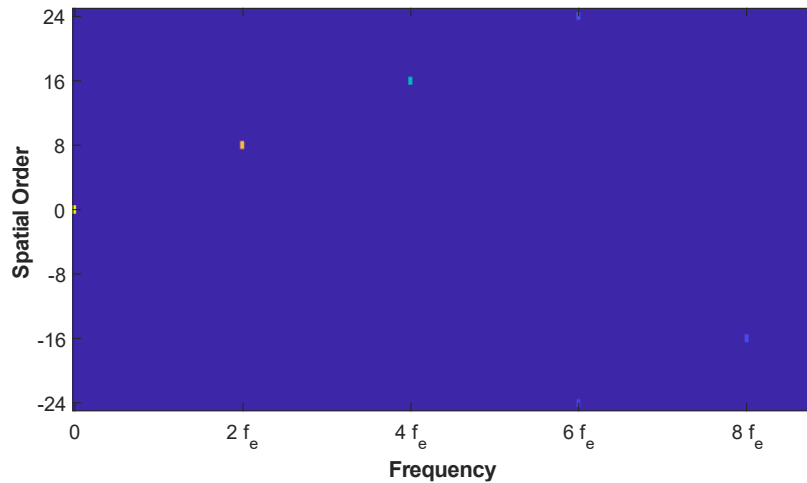


Figure 3 - 2D Fourier Decomposition of the stator forces

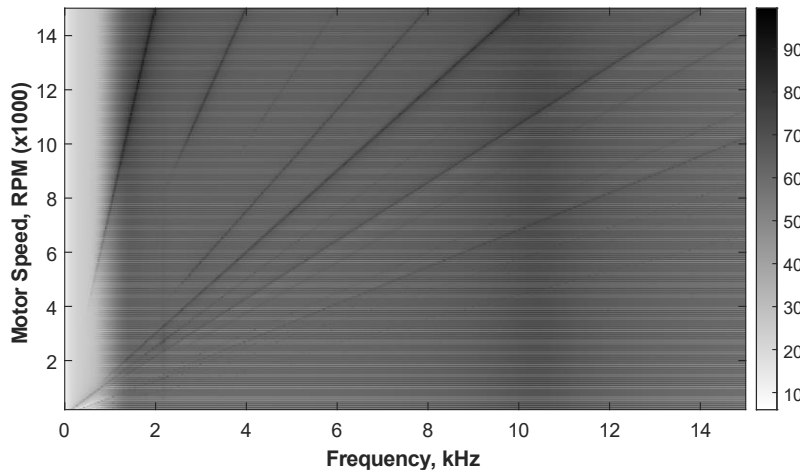


Figure 4 - Sound Pressure Levels for Open Circuit speed-sweep (0-15,000 RPM)

4. CONCLUSIONS

In this paper, a reduced order methodology for predicting the electromagnetic noise generation of a typical traction S-PMSM has been presented. Unlike numerical approaches widely used in literature, the use of analytical modelling techniques allows for a fast prediction of the electromagnetic and vibroacoustic behaviour of such a system that can be of crucial importance in early design stages. The analytical expressions enable for characterisation of the electromagnetic force harmonics, hence allowing for a deeper understanding of the noise origins. Finally, the computational efficiency of the model relative to numerical techniques allows for quick parametric studies to be performed in pre-design stages, such that low-noise design rules can be defined, and their effects on other aspects of the motor's performance to be evaluated/

ACKNOWLEDGMENTS

The authors would like to express their gratitude to the Engineering and Physical Sciences Research Council (EP/T518098/1 – Electric motor and transmission coupled vibro-acoustics of electric powertrains), to the Engineering and Physical Sciences Research Council (EP/V053353/1 – Automotive electric powertrain whistling and whining: fundamental root cause analysis to novel solutions) and to the Loughborough University Doctoral College for their support.

REFERENCES

- [1] 'New UK EV and AFV Registrations - SMMT monthly data'. <https://www.smmt.co.uk/vehicle-data/evs-and-afvs-registrations/> (accessed Jul. 04, 2022).
- [2] J. F. Gieras, C. Wang, and J. Cho Lai, 'Generation and Radiation of Noise in Electrical Machines', in *Noise of Polyphase Electric Motors*, 1st ed., CRC Press, 2006, pp. 1–20.
- [3] E. Devillers, 'Electromagnetic subdomain modeling technique for the fast prediction of radial and circumferential stress harmonics in electrical machines', Centrale Lille, Lille, 2018.
- [4] J. B. Dupont and P. Bouvet, 'Multiphysics Modelling to Simulate the Noise of an Automotive Electric Motor', *SAE Technical Papers*, Jun. 2012, doi: 10.4271/2012-01-1520.
- [5] X. Liang, G. Li, J. Ojeda, M. Gabsi, and Z. Ren, 'Comparative study of classical and mutually coupled switched reluctance motors using multiphysics finite-element modeling', *IEEE Transactions on Industrial Electronics*, vol. 61, no. 9, pp. 5066–5074, 2014, doi: 10.1109/TIE.2013.2282907.
- [6] Z. Yang, F. Shang, I. P. Brown, and M. Krishnamurthy, 'Comparative study of interior permanent magnet, induction, and switched reluctance motor drives for EV and HEV applications', *IEEE Transactions on Transportation Electrification*, vol. 1, no. 3, pp. 245–254, Oct. 2015, doi: 10.1109/TTE.2015.2470092.
- [7] Y. S. Wang, H. Guo, T. Yuan, L. F. Ma, and C. Wang, 'Electromagnetic noise analysis and optimization for permanent magnet synchronous motor used on electric vehicles', *Engineering Computations (Swansea, Wales)*, vol. 38, no. 2, pp. 699–719, Feb. 2021, doi: 10.1108/EC-02-2020-0070/FULL/PDF.
- [8] F. L. M. dos Santos, J. Anthonis, F. Naclerio, J. J. C. Gyselinck, H. van der Auweraer, and L. C. S. Góes, 'Multiphysics NVH modeling: Simulation of a switched reluctance motor for an electric vehicle', *IEEE Transactions on Industrial Electronics*, vol. 61, no. 1, pp. 469–476, 2014, doi: 10.1109/TIE.2013.2247012.
- [9] M. Islam, R. Islam, and T. Sebastian, 'Noise and vibration characteristics of permanent magnet synchronous motors using electromagnetic and structural analyses', *IEEE Energy Conversion Congress and Exposition: Energy Conversion Innovation for a Clean Energy Future, ECCE 2011, Proceedings*, pp. 3399–3405, 2011, doi: 10.1109/ECCE.2011.6064228.

- [10] P. Pellerey, V. Lanfranchi, and G. Friedrich, 'Numerical simulations of rotor dynamic eccentricity effects on synchronous machine vibrations for full run up', *Proceedings - 2012 20th International Conference on Electrical Machines, ICEM 2012*, pp. 3008–3014, 2012, doi: 10.1109/ICELMACH.2012.6350316.
- [11] J. Feng, J. Deng, Y. Liu, H. Hou, and R. Oka, 'The Resolution of 8th Order Whining Noise for a Battery Electric Vehicle', *SAE Technical Papers*, vol. 2020-April, no. April, Apr. 2020, doi: 10.4271/2020-01-1269.
- [12] S. Arabi, G. Steyer, Z. Sun, and J. Nyquist, 'Vibro -Acoustic Response Analysis of Electric Motor', *SAE Technical Papers*, vol. 2017-June, no. June, Jun. 2017, doi: 10.4271/2017-01-1850.
- [13] G. He, Z. Huang, R. Qin, and D. Chen, 'Numerical prediction of electromagnetic vibration and noise of permanent-magnet direct current commutator motors with rotor eccentricities and glue effects', *IEEE Trans Magn*, vol. 48, no. 5 PART 2, pp. 1924–1931, May 2012, doi: 10.1109/TMAG.2011.2178100.
- [14] E. Devillers, P. Gning, and J. le Besnerais, 'Effect of uneven magnetization on magnetic noise and vibrations in PMSM - Application to EV HEV electric motor NVH', in *Proceedings - 2020 International Conference on Electrical Machines, ICEM 2020*, Aug. 2020, pp. 1786–1792. doi: 10.1109/ICEM49940.2020.9270988.
- [15] J. B. Dupont, R. Aydoun, and P. Bouvet, 'Simulation of the noise radiated by an automotive electric motor: Influence of the motor defects', *SAE International Journal of Alternative Powertrains*, vol. 3, no. 2, pp. 310–320, Jul. 2014, doi: 10.4271/2014-01-2070.
- [16] Z. Q. Zhu and D. Howe, 'Instantaneous magnetic field distribution in brushless permanent magnet dc motors, Part III: Effect of stator slotting', *IEEE Trans Magn*, vol. 29, no. 1, pp. 143–151, 1993, doi: 10.1109/20.195559.
- [17] Z. Q. Zhu, Z. P. Xia, L. J. Wu, and G. W. Jewell, 'Analytical modelling and finite element computation of radial vibration force in fractional-slot permanent magnet brushless machines', *2009 IEEE International Electric Machines and Drives Conference, IEMDC '09*, pp. 144–151, 2009, doi: 10.1109/IEMDC.2009.5075197.
- [18] M. Wang, J. Zhu, L. Guo, J. Wu, and Y. Shen, 'Analytical Calculation of Complex Relative Permeance Function and Magnetic Field in Slotted Permanent Magnet Synchronous Machines', *IEEE Trans Magn*, vol. 57, no. 3, Mar. 2021, doi: 10.1109/TMAG.2020.3046354.
- [19] J. F. Gieras, C. Wang, and J. Cho Lai, 'Magnetic Fields and Radial Forces in Polyphase Motors Fed with Sinusoidal Currents', in *Noise of Polyphase Electric Motors*, 1st ed., vol. 1, M. O. Thurston, Ed. Ohio: Taylor & Francis Group, LLC, 2006, pp. 21–64.
- [20] J. F. Gieras, C. Wang, and J. Cho Lai, 'Stator System Vibration Analysis', in *Noise of Polyphase Electric Motors*, 1st ed., vol. 1, M. O. Thurston, Ed. Ohio: Taylor & Francis Group, LLC, 2006, pp. 107–126.
- [21] J. le Besnerais, 'Reduction of magnetic noise in PWM-supplied induction machines-low-noise design rules and multi-objective optimization', Laboratoire d'Electricité et d'Electronique de Puissance de Lille, Lille, 2008. [Online]. Available: <https://tel.archives-ouvertes.fr/tel-00348730>